Journal of Molecular Structure 1019 (2012) 166–173

Contents lists available at SciVerse ScienceDirect

Journal of Molecular Structure

journal homepage: www.elsevier.com/locate/molstruc

FT-IR, FT-Raman and fluorescence studies of Tb^{3+} ions activated lead containing sodium fluoroborate glasses

C. Madhukar Reddy [a], B. Sudhakar Reddy [c], G.R. Dillip [a], K. Mallikarjuna [a], B. Deva Prasad Raju [b,*]

[a] Department of Physics, Sri Venkateswara University, Tirupati 517 502, India
[b] Department of Future Studies, Sri Venkateswara University, Tirupati 517 502, India
[c] Department of Physics, Sri Venkateswara Degree College, Kadapa 516 003, India

ARTICLE INFO

Article history:
Received 9 December 2011
Received in revised form 26 February 2012
Accepted 27 February 2012
Available online 7 March 2012

Keywords:
Glasses
FT-Raman
Oscillator strengths
J–O parameters
Fluorescence
Lifetimes

ABSTRACT

This study reports on the concentration dependent fluorescence properties of Tb^{3+}-doped lead containing calcium zinc sodium fluoroborate (LCZSFB) glasses and are analyzed by DSC, FT-IR, FT-Raman, optical absorption, emission and decay curve spectra. Co-existence of trigonal BO_3 and tetrahedral BO_4 units was evidenced by FT-IR and Raman spectroscopy. Judd–Ofelt theory was applied to the experimental oscillator strengths to evaluate the J–O intensity parameters. The fluorescence spectra of Tb^{3+}-doped glasses have revealed prominent blue and green emissions originating from $^5D_3$ and $^5D_4$ excited levels to ^7F_J ground state multiplet, respectively. The luminescent intensity of the transitions originating from $^5D_4$ state increases with increase of Tb^{3+} concentration and no quenching effect is noticed up to 2 mol% of Tb^{3+} ions. Chromaticity color coordinates have been calculated and the dominant emission in the green region is discussed. The nature of decay curves of $^5D_4$ level for different Tb^{3+} ion concentration in all LCZSFB glasses has been analyzed. Using the J–O intensity parameters as well as from the emission and decay curve measurements, various radiative and fluorescence properties have been calculated for the $^5D_4$ fluorescent level. Based on these results, the utility of Tb^{3+} ions doped LCZSFB glasses as laser active materials for high intensity emissions in the green region is discussed.

1. Introduction

In the area of photonics rare earth ions doped glasses have received much attention, because of their high potential applications as laser hosts, tunable waveguides, etc. The fluorescence originating from f–f transitions of rare earth ions activated in glasses, also due to the high quantum efficiencies and very narrow fluorescence bands of rare earths in different glass hosts is main reason of interest for practical photonic device applications. Glasses offer medium for the production of most compact and efficient devices and also from the literature it is clear that these optical glasses when doped with certain rare earth ions, could display hopeful and significant optical results in optical communication fibers, solid state lasers, light converters, sensors, etc. [1–6]. Rare earth ions doped glasses are promising for active display and image processing panels due to their transparent, easy shaping and cost effective properties. Compared with phosphors luminescent glasses have some advantages when used in the preparation of LED such as lower fabrication cost and simpler manufacture procedure. Therefore luminescent glasses could be considered as good alternatives for LED [7,8]. Stimulated research and development of new scintillating materials is required due to huge demand in the applications of scintillators in high-energy and nuclear physics, medical imaging industry, etc.

Selection of glass host and the active ion concentration is more important to be considered in developing more efficient optical devices based on rare earth ions. The host matrix should have low phonon energy to minimize the multi phonon relaxation rates due to less energy difference between the energy levels. Oxide glasses are attracting hosts for obtaining efficient luminescence in rare earth ions. Among them borate glasses have attracted much attention because of their electrochemical and optical applications such as solid state batteries, optical wave guides and luminescent materials [9,10]. Moreover borate glasses are important hosts for rare earth ions because of their chemical durability and better mechanical properties, but at the same time the rare earth ion emissions are strongly reduced due to their higher lattice vibrations. To avoid this problem, the glasses with low phonon energies such as fluorides, tellurites, germinates and heavy metal oxide glasses are required. Lead containing glasses are more promising for photonics and optoelectronics. Depending on ionic or covalent bond between lead and oxide, PbO plays the role as a modifier or a glass former [9]. Based upon these findings, one can expect that the incorporation of PbO into the borate matrix will influence significantly the structure and glass properties because of extremely

* Corresponding author. Tel.: +91 94402 81769.
E-mail address: drdevaprasadraju@gmail.com (B. Deva Prasad Raju).

0022-2860/$ - see front matter © 2012 Elsevier B.V. All rights reserved.
doi:10.1016/j.molstruc.2012.02.066

large difference between the masses of the lead and the boron atoms [9,11,12]. The structure of the borate glass is a random mixture of different borate groups formed by the gathering of the BO_3 and BO_4 structural units and concentration of modifier ion also plays a significant role in the presence of different groups [13]. In addition the lead borate optical glasses are excellent hosts to incorporate trivalent rare earth ions due to their optical transparency from the visible to NIR range, forming over a wide compositional region of PbO concentration and also due to the large difference between the masses of the lead and the boron atoms are favorable for spectroscopic studies. Due to their high transparency and relatively low phonon energies fluoride glasses are of special importance in the development of high performance new materials for infrared optical applications. These glasses are considered as active optoelectronic materials. Among the oxyfluoride glasses that have been investigated so far, particular attention has been devoted to the fluoroborate glasses as they combine both the advantages of fluoride and borate glasses, such as low phonon energy, good moisture resistance, physical and chemical stability, high transparency, low melting point, easy shaping and cost effective properties. These features characterize them as potential laser active media [14–16] in the visible and NIR spectral regions and these advantages are useful for structural and optical investigations in oxyfluoride lead borate glasses.

Among the various rare earth ions, it is well known that the Tb^{3+} ions doped glasses are of particular interest due to their wide applications in various fields of photonics such as in the development of efficient green emitting phosphors in fluorescent lamps for display applications, projection television tubes, X-ray intensifying screens and scintillating materials. The long spontaneous emission lifetimes and narrow spectral widths of the green emission and high quantum efficiency make Tb^{3+} based molecules an ideal choice for biological probes [17]. Terbium doped scintillating materials have been extensively used in many applications such as thermal neutron detection and radiography, non destructive testing. Generally the luminescence spectrum of Tb^{3+} is very complicated and due to the $4f^8$ orbital of Tb^{3+}, it requires comparatively little energy in UV region to excite the ground state to the 5d state. Its emission mainly originates from $^5D_4$ and $^5D_3$ to ^7F_J (J = 0–6) levels [18–20]. Tb^{3+} ion provide the information about the clustering of rare earth ions and convenient means of understanding the nature of metal coordination in various systems. As a result of well isolated ^7F_J multiplet states and the large energy gap between these states and the emitting level, the luminescence property of Tb^{3+} has been proven to be useful in characterizing the energy level structure and optical transmission process.

In this paper, the spectroscopic properties of different concentrations of terbium doped LCZSFB glasses have been investigated by using the DSC, FT-IR, FT-Raman, optical absorption, photoluminescence and decay measurements.

2. Experimental methods

LCZSFB glasses of $20PbO + 5CaO + 5ZnO + 10NaF + (60 - x)B_2O_3 + xTb_2O_3$, (where x = 0.1, 0.5, 1.0, 1.5 and 2.0 mol%) were prepared. The approximate quantities of reagent grade chemicals were powdered homogeneously and melted in an electric furnace at 950 °C about one hour using porcelain crucible. The melt was poured onto a pre-heated brass mould and annealed at 360 °C for 8 h to remove thermal strains acquired by the glass matrix during sudden quenching. The glass samples were slowly cooled to room temperature, shaped and polished to measure their physical and optical properties. Densities of glass samples were (5.19 g/cm^3) were measured at room temperature with distilled water as the immersion liquid by the conventional Archimedes's principle. Abbe's refractometer was used to obtain the refractive indices (~1.588) for all the glass samples at sodium wavelength using 1-bromonapthlene as the contact liquid. The various measured and calculated physical properties of the 1.0 mol% Tb^{3+}-doped LCZSFB glasses are presented in Table 1.

Differential scanning calorimeter profile is recorded on a Netzsch DSC 204 differential scanning calorimeter in the temperature range of 0-500 °C, at the rate of 10 °C/min, under N_2 gas atmosphere. FT-IR spectrum in the range 450–4000 cm^{-1} using Perkin–Elmer Spectrum One FTIR spectrophotometer by the standard KBr pellet technique was recorded. FT-Raman spectra in the range 50–5000 cm^{-1} with Bruker RFS 27 stand alone Raman spectrometer using 1064 nm light from Nd:YAG laser on glass powders were recorded in black scattering geometry with a resolution of 2 cm^{-1}. The absorption spectra were recorded using a double beam Perkin Elmer Lambda 950 spectrophotometer in the wavelength range 250–2500 nm. The excitation, emission and lifetime measurements were carried out using Jobin Yvon Fluorolog-3 spectrofluorometer with xenon flash lamp as source. All the measurements were carried out at room temperature.

3. Results and discussion

3.1. Thermal studies

The DSC thermogram of 1.0 mol% of Tb^{3+}-doped LCZSFB glass is shown in Fig. 1. From this figure it is observed that the glass transition temperature (T_g) of the sample is at around 478 °C. The glass transition temperature is related to the density of cross linking, the number and strength of the coordinate links formed between oxygen atoms and the cation, and the oxygen density of the network. Higher values of this factor correspond to higher T_g. The value of T_g strongly depends on O/F ratio in glass composition. Introduction of the oxide component to the fluoride matrix introduces an increase of glass transition temperature, which is attributed to the formation of stronger chemical bonds [21,22]. The endothermic peak at around 225 °C is related to the loss of OH and the decomposition of hydroxide.

3.2. Vibrational studies

3.2.1. Infrared spectroscopy

FT-IR and FT-Raman spectroscopy represent two intensively employed techniques for study the structural details of the vitreous systems. Having different selection rules, these two spectroscopic techniques prove to be very powerful complementary methods in revealing the glass structure. The structure of vitreous borate consists of a random network of BO_3 triangles with certain

Table 1
Measured and calculated physical properties of 1.0 mol% Tb^{3+}-doped LCZSFB glass.

Physical quantities	LCZSFB
Sample thickness (cm)	0.280
Refractive index, n	1.588
Density (g/cm^3)	5.190
Concentration (mol/l)	0.272
Concentration (ions cm^{-3} × 10^{20})	1.640
Average molecular weight (g)	187.300
Dielectric constant, ε	2.522
Molar volume, V_m (cm^3/mol)	36.088
Glass molar refractivity (cm^{-3})	12.146
Electronic polarizability, α_e (×10^{-24} cm^3)	4.820
Reflection losses, R (%)	5.162
Polaron radius, r_p (A°)	7.360
Inter ionic distance, r_i (A°)	18.230
Field strength, F (×10^{14} cm^{-2})	5.500
Glass transition temperature, T_g (°C)	478

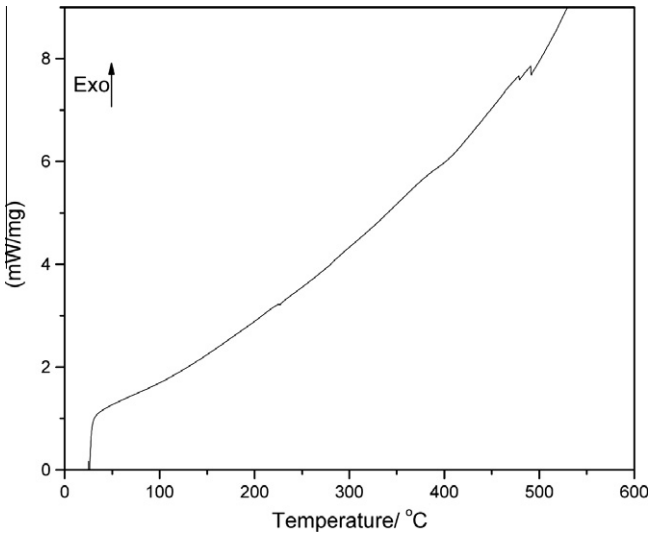

Fig. 1. DSC profile of 1.0 mol% Tb^{3+}-doped LCZSFB glass.

fraction of boroxol rings but with the inclusion of the network modifiers, formation of BO_4 tetrahedra takes place in the borate glass network. The FT-IR spectrum of 1.0 mol% Tb^{3+}-doped LCZSFB glass in the IR region 450–4000 cm^{-1} is shown in Fig. 2. The peak at 495 cm^{-1} could be due to loose BO_4 units [23]. The bands at 707 and 975 cm^{-1} could be due to the bending and stretching vibrations of BO_4, while the peak around 1319 cm^{-1} is due to B–O stretching vibrations of BO_3 units [24]. The peak around 1631 cm^{-1} may be due to asymmetric stretching relaxation of the B–O bond of trigonal BO_3 units [25]. Similarly the well known peaks in the region 2700–3500 cm^{-1} are due to OH bond vibrations [25]. In general, the band at 806 cm^{-1} is assigned to the boroxol ring in the pure borate glass network. In the present study, the peak at 806 cm^{-1} is found to be missing, which indicates the absence of a boroxol ring in the glass network. The vanishing of band at 806 cm^{-1} means no boroxol ring in the glass structure and the progressive substitution of boroxol rings by tri-borate (BO_3) and tetra-borate (BO_4) groups are observed.

3.2.2. Raman spectroscopy

The FT-Raman spectrum of 1.0 mol% Tb^{3+}-doped LCZSFB glass in the region 0–2000 cm^{-1} is shown in Fig. 3. The asymmetric and depolarized Raman band at 89 cm^{-1} is named as boson peak and is associated to the BO_3–PbO_4 bridged local collective vibrations [26,27]. The 475 cm^{-1} band is assigned to a ring angle bending (B–O–B), which is observed at 470 cm^{-1} for pure B_2O_3 [28]. The bands located at 635 and 720 cm^{-1} are related to the chain and ring type metaborate groups [26,29,30]. The occurrence of band at around 903 cm^{-1} is an indication of the presence of pentaborate groups in the borate glasses [26,30]. The band centered at 1269 cm^{-1} is assigned to pyroborate groups [26,28,29,31]. The bands in the region 1300–1600 cm^{-1} is similar to that in the Raman spectra of large number of modifier borate glasses. These bands have been assigned to the stretching of $B–O^-$ stretching in metaborate rings and chains [28,29,31]. The absence of Raman band at 805 cm^{-1} also confirms the absence of borxol rings in the present LCZSFB glass which is already identified from FT-IR spectra of Fig. 2.

3.3. Optical absorption spectra

The optical absorption spectra of 1.0 mol% Tb^{3+}-doped LCZSFB glass recorded at room temperature in the visible region 450–550 nm and in near infrared region 1500–2500 nm are shown in Figs. 4 and 5 respectively. The absorption spectra contain four bands centered at 485, 1894, 1953 and 2206 nm corresponding to $^7F_6 \rightarrow {}^5D_4$, $^7F_1$, $^7F_2$ and $^7F_3$ transitions, respectively. The assignment of absorption transitions has been done based on the earlier literature [32]. All the absorption transitions in the spectra are originate from induced electric dipole interactions following the selection rules, $\Delta S = 0$, $|\Delta L| \leqslant 6$, $|\Delta J| \leqslant 6$ [33]. Among these absorption transitions, the $^7F_6 \rightarrow {}^5D_4$ transition located in the visible region (Fig. 4) is very weak and the other transitions $^7F_6 \rightarrow {}^7F_J$ ($J = 1, 2$ and 3) located in the near infrared region (Fig. 5) are more intense. The absorption peaks in the visible region are very poor. This is not only in the present oxy fluoroborate glass matrix even in other glass matrices too the absorption spectra of Tb^{3+} are very weak and only a few peaks could be observed.

3.4. Oscillator strengths: Judd–Ofelt analysis

The spectral intensities of the observed absorption transitions are expressed in terms of oscillator strengths. From the absorption spectra the experimental oscillator strengths (f_{exp}) are determined

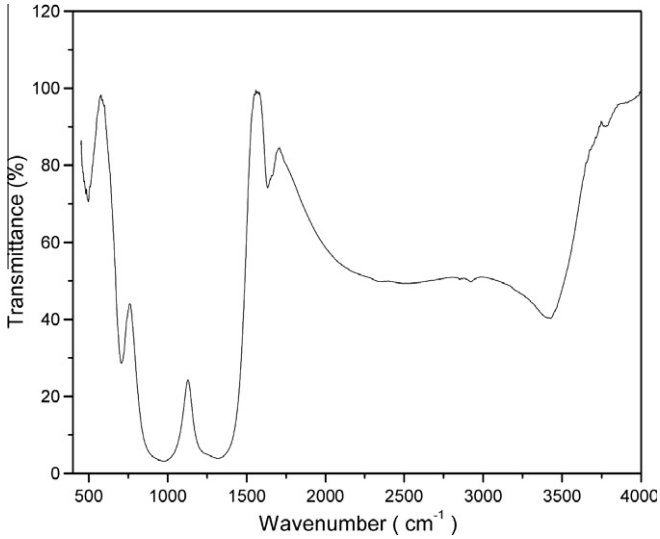

Fig. 2. FT-IR spectrum of 1.0 mol% Tb^{3+}-doped LCZSFB glasses.

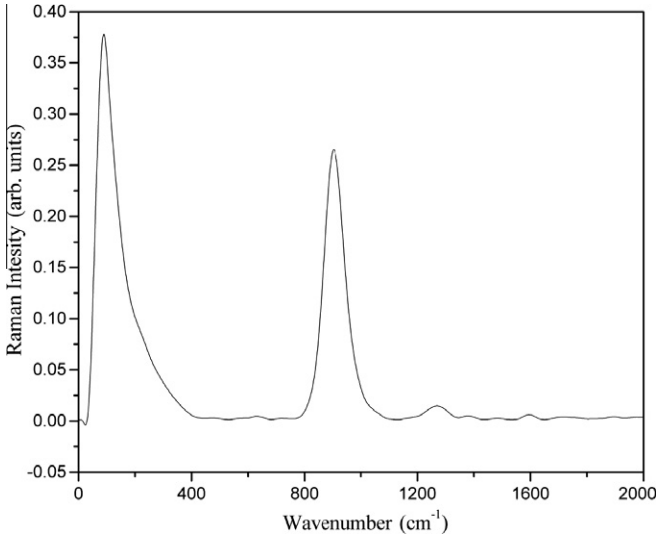

Fig. 3. FT-Raman spectrum of 1.0 mol% Tb^{3+}-doped LCZSFB glasses.

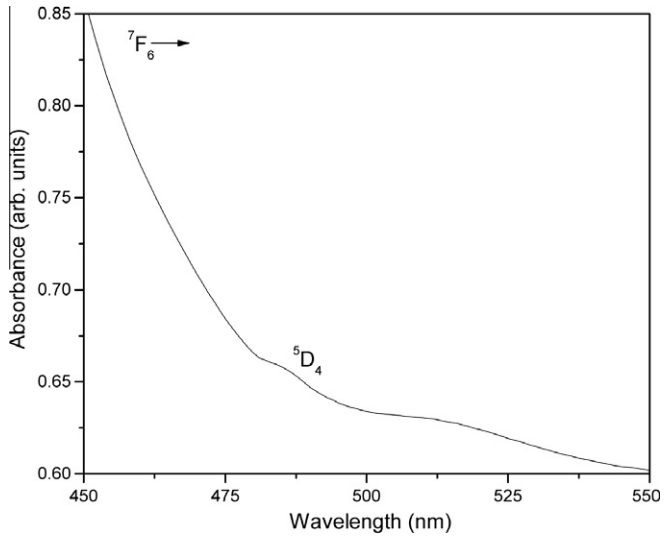

Fig. 4. Vis absorption spectra of 1.0 mol% Tb^{3+}-doped LCZSFB glasses.

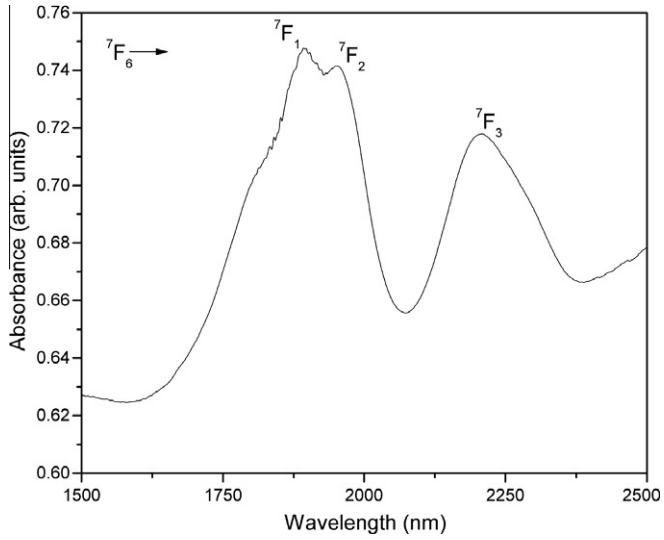

Fig. 5. NIR absorption spectra of 1.0 mol% Tb^{3+}-doped LCZSFB glasses.

by measuring the areas under the $^5D_4$, $^7F_1$, $^7F_2$ and $^7F_3$ transitions arising from the $^7F_6$ ground state, using the equation

$$f_{exp} = \frac{2.303mc^2}{N\pi e^2}\int \varepsilon(v)dv = 4.318\times 10^{-9}\int \varepsilon(v)dv \quad (1)$$

The Judd–Ofelt intensity parameters were calculated using the experimental values of oscillator strengths (f_{exp}) and the reduced matrix elements by the least-square-fit method. The calculated oscillator strengths, f_{cal} of electric dipole transitions between an initial state ΨJ and final state $\Psi' J'$ with in the $4f^8$ configuration can be determined by least-square-fit procedure using f_{exp} values and the J–O intensity parameters Ω_λ (λ = 2, 4, 6) from the following equation [34,35].

$$f_{cal} = \frac{8\pi^2 mc\nu}{3h(2J+1)}\frac{(n^2+2)^2}{9n}\sum_{\lambda=2,4,6}\Omega_\lambda(\Psi J||U^\lambda||\Psi' J')^2 \quad (2)$$

The reduced matrix elements $||U^\lambda||$ which are insensitive to the ion environments were taken from Carnall et al. [32]. The absorption transitions, their peak positions, experimental and calculated oscillator strengths are given in Table 2. The magnitude of oscillator strengths of $^7F_6 \rightarrow {}^7F_J$ (J = 1, 2 and 3) absorption transitions indicates that these three transitions are more intense in 1.0 mol% Tb^{3+}-doped LCZSFB glass. The quality of the fit between the experimentally determined (f_{exp}) and theoretically calculated (f_{cal}) oscillator strengths can be expressed by root mean square deviation (δ_{rms}). The δ_{rms} value of $\pm 0.076 \times 10^{-6}$ shows a good fit between f_{exp} and f_{cal} values and also the validity of J–O intensity parameters.

Judd–Ofelt theory is the most suitable theory to characterize the intensities of forced electric dipole transitions between 4f states of lanthanide ions. The host matrix dependent electric-dipole absorption transitions are quantified using the Judd–Ofelt theory [34,35] and the J–O intensity parameters evaluated for glass. The evaluated J–O intensity parameters are compared in Table 3 along with the values reported for various other glass hosts doped with Tb^{3+} ions [36–39]. The J–O intensity parameters are found in the order $\Omega_2 > \Omega_6 > \Omega_4$ for all the host matrices. From magnitudes of Ω_λ, it is noticed that Ω_2 is extremely sensitive due to the configuration admixing, where as Ω_4 and Ω_6 are less sensitive to the local environment of the Tb^{3+} in any glass system. The J–O parameters can provide a view of the field strength of hosts. The higher values of Ω_λ and oscillator strengths obtained in the present case compared to those may be attributed to a stronger field and lower site symmetry of rare-earth ions in the glass. In general the Ω_2 is strongly influenced by covalency of metal ligand bonding and explains the asymmetry of ion sites in the vicinity of RE ions. In general, the lesser the Tb–O average distance, the stronger is the field around the Tb^{3+} ion that lead to a high value of Ω_2. Reasonably high value of Ω_2 results the increase of covalent bonding and suggests that the RE ion site has lower symmetry in LCZSFB glass host. On the other hand Ω_4 and Ω_6 values depend on the bulk properties such as viscosity and rigidity of the media and are also strongly influenced by the vibrational levels associated with the central Tb^{3+} ions bound to the ligand atoms [40,41].

3.5. Excitation and emission spectra

Fig. 6 represents the excitation spectrum of 1.0 mol% Tb^{3+}-doped LCZSFB glass monitored by the emission at 547 nm corresponding to $^5D_4 \rightarrow {}^7F_5$ emission level recorded in the region 300–500 nm. It contains five excitation transitions, out of which one band ($^7F_6 \rightarrow {}^5D_4$) is already identified in absorption spectrum at a wavelength of 485 nm (Fig. 4) and the remaining four bands noticed at 318, 352, 370 and 378 nm corresponding to $^7F_6 \rightarrow {}^5D_1$, $^5L_9$, $^5L_{10}$, and $^5G_6$ transitions are the hidden bands in the absorption spectra due to intrinsic absorption of the host glass matrix.

When Tb^{3+} ions are excited by the UV wavelengths, electronic transitions of either $^5D_3 \rightarrow {}^7F_J$ (J = 6, 5, 4, 3) (blue emission) or successive $^5D_3 \rightarrow {}^5D_4$ and $^5D_4 \rightarrow {}^7F_J$ (J = 6, 5, 4, 3) (green emission) would takes place [42]. In the case of Tb^{3+}-doped glass hosts, the emissions below 480 nm originate from $^5D_3$ level and the emissions above 480 nm originate from $^5D_4$ levels. Fig. 6 represents the emission spectra originated from $^5D_4$ excited state for different concentrations of Tb^{3+}-doped LCZSFB glasses obtained with the

Table 2
Experimental and calculated oscillator strengths ($\times 10^{-6}$) for 1.0 mol% Tb^{3+}-doped LCZSFB glass.

Transition		Energy (cm^{-1})	f_{exp}	f_{cal}
$^7F_6 \rightarrow$	$^5D_4$	20,619	0.05	0.05
	$^7F_1$	5280	1.19	0.97
	$^7F_2$	5120	0.97	1.18
	$^7F_3$	4533	0.98	0.94
			$\delta_{rms} = \pm 0.076 \times 10^{-6}$	

Table 3
Comparison of J–O intensity parameters ($\times 10^{-20}$ cm^2), their trends for Tb^{3+} ions in LCZSFB glass with different glass hosts.

Glass system	Ω_2	Ω_4	Ω_6	Trend
LCZSFB [present glass]	14.54	0.17	4.09	$\Omega_4 > \Omega_6 > \Omega_2$
Fluoride glass [36]	13.40	2.15	4.90	$\Omega_4 > \Omega_6 < \Omega_2$
$KF–B_2O_3$ [37]	11.92	0.26	2.16	$\Omega_4 > \Omega_6 > \Omega_2$
$LiNO_3–KNO_3$ [38]	15.00	2.86	5.24	$\Omega_4 > \Omega_6 > \Omega_2$
$Li_2O–B_2O_3$ [39]	05.56	1.33	3.22	$\Omega_4 > \Omega_6 > \Omega_2$

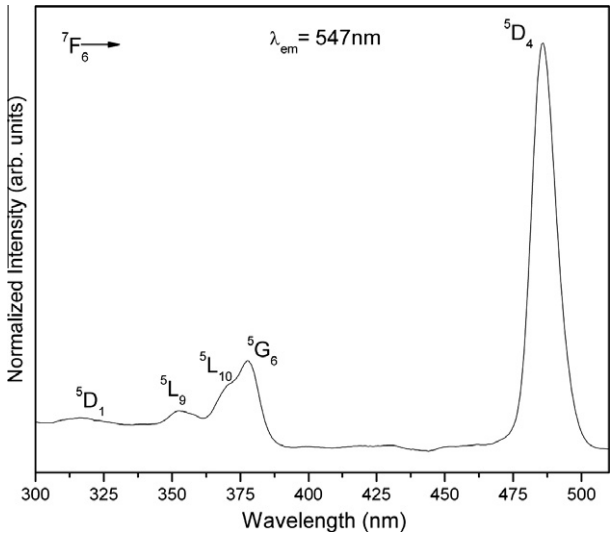

Fig. 6. Excitation spectrum of 1.0 mol% Tb^{3+}-doped LCZSFB glasses.

excitation wavelength of 378 nm. In general, Tb^{3+} ions exhibit strong fluorescence in blue and green spectral regions corresponding to the $^5D_4 \rightarrow {}^7F_6$ and $^7F_5$ transitions, respectively. The emission spectra in the region 450–650 nm originating from $^5D_4$ state (Fig. 7) contain four peaks at 492, 547, 588 and 623 nm assigned to $^5D_4 \rightarrow {}^7F_6$, $^7F_5$, $^7F_4$ and $^7F_3$ transitions respectively with in the $4f^8$ configuration of the Tb^{3+} ions. Among the four intense transitions the green fluorescence at 547 nm corresponding to $^5D_4 \rightarrow {}^7F_5$ transition is the most intense one. The intense green emission at 547 nm arises from the Laporte-forbidden $^5D_4 \rightarrow {}^7F_5$ transition [43,44]. The transition $^5D_4 \rightarrow {}^7F_6$ is the magnetic dipole transition and obeys the selection rule of $\Delta J = \pm 1$ [45,46]. The fluorescence intensity of the observed transitions increases gradually with the increase of Tb^{3+} ion concentration from 0.1 to 2.0 mol% for the emissions originating from $^5D_4$ state and no fluorescence quenching has been observed. This may be due to large energy gap ($\sim$14,000 cm^{-1}) and absence of cross-relaxation channels. Hence, one can conclude that the intensity of luminescence can be further increased by increasing the Tb^{3+} ion concentration in LCZSFB glasses.

Inset of Fig. 7 represents the fluorescence spectra of $^5D_3$ excited state. The emission from the excited $^5D_3$ state has been reported by several researchers [42,47–52]. Three peaks are identified at 418, 442 and 458 nm corresponding to $^5D_3 \rightarrow {}^7F_5$, $^7F_4$ and $^7F_3$ transitions respectively. Based on the energies of different transitions obtained from the absorption, excitation and emission spectra the energy level diagram drawn for Tb^{3+} ions in LCZSFB glass is shown in Fig. 8. From the energy level diagram it is observed that the energy gap between the $^5D_3$ and $^5D_4$ levels is equal to the energy difference with in the ^7F_J (J = 0–6) multiplets. The energy level diagram also shows different emission transitions observed from the $^5D_4$ and $^5D_3$ states as indicated in Fig. 8.

3.6. Luminescence analysis and radiative properties

The fluorescence characteristics of $^5D_4$ manifold of Tb^{3+} in LCZSFB glasses have been predicted by evaluating the radiative properties. The evaluated J–O parameters are used to predict the radiative properties for the electric dipole transitions between any excited level (ΨJ) to its lower lying level ($\Psi' J'$). The radiative transition probability (A_R) for emission from an initial state ΨJ to a final state $\Psi' J'$ can be expressed as

$$A_R(\Psi J, \Psi' J') = \frac{64\pi^4 v^3}{3h(2J+1)}\left[\frac{n(n^2+2)^2}{9}S_e d + n^3 S_{md}\right] \quad (3)$$

The radiative lifetime (τ_R) of an excited state is given by

$$\tau_R(\Psi J) = \frac{1}{\sum_{\Psi' J'} A_R(\Psi J, \Psi' J')} \quad (4)$$

The branching ratios (β_R) corresponding to the emission from an excited level ΨJ to its lower level $\Psi' J'$ are given by

$$\beta_R(\Psi J, \Psi' J') = \frac{A_R(\Psi J, \Psi' J')}{\sum_{\Psi' J'} A_R(\Psi J, \Psi' J')} \quad (5)$$

The peak stimulated emission cross section σ_e (ΨJ, $\Psi' J'$), between the emission levels ΨJ and $\Psi' J'$ having probability of A_R (ΨJ, $\Psi' J'$) can be expressed as

$$\sigma_e(\Psi J, \Psi' J') = \frac{\lambda_p^4}{8\pi c n^2 \Delta\lambda_p} A_R(\Psi J, \Psi' J') \quad (6)$$

where λ_p is the peak wave length and $\Delta\lambda_p$ is the effective line width, found by dividing the area of the emission band by its average height.

As the magnetic dipole contribution is negligible, only the electric dipole transitions are taken into consideration and the electric dipole line strengths (S_{ed}) corresponding to the transitions from the upper manifold state $^5D_4$ to the lower manifold states ^7F_J (J = 0–6) have been determined using the following equation

$$S_{ed} = e^2 \sum_{\lambda=2,4,6} \Omega_\lambda (\Psi J || U^\lambda || \Psi' J')^2 \quad (7)$$

The radiative transition rates (A_R), effective emission band widths ($\Delta\lambda_p$), branching ratios (β_R), measured branching ratios (β_m) and stimulated emission cross sections (σ_e) have been determined for the $^5D_4$ level of 1.0 mol% Tb^{3+}-doped and are presented in Table 4. The fluorescent properties such as measured branching ratios (β_m), lifetimes (τ_m), stimulated emission cross sections (σ_e), optical gain parameters ($\sigma_e \times \tau_m$) and quantum efficiencies (η) are of important to select a good laser host material.

From the values of radiative transition probabilities of Table 4, it is noticed that $^5D_4 \rightarrow {}^7F_5$ has highest radiative transition rate compared to other transitions. Hence this transition is very useful for laser emission. The predicted branching ratios are found to be high for those transitions having maximum A_R values. The levels having the relatively large values of A_R, β_R and energy gap to the next lower level may exhibit laser action. The measured branching ratios of three emission transitions $^5D_4 \rightarrow {}^7F_J$ (J = 4–6) were found to be nearly 4%, 55% and 40% respectively. The contribution of these transitions to the total branching ratio is nearly 99%, there by suggesting that these transitions have the most potential for visible laser action for 1.0 mol% Tb^{3+} ions in LCZSFB glasses. In practice, the most potential laser transitions possess large values of stimulated emission cross sections [53]. In the present investigation, $^5D_4 \rightarrow {}^7F_5$ transition posse's highest magnitude of stimulated emission cross section of 15.46×10^{-22} cm^2 which is comparable to other reported values [36,37,52,54–56]. Such a trend encourages for green

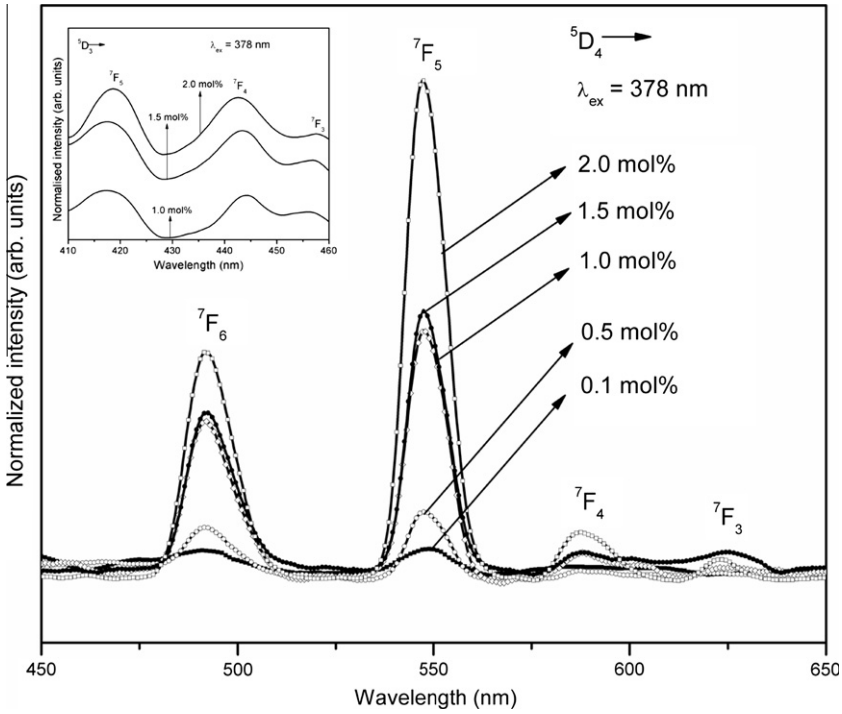

Fig. 7. Fluorescence spectra of $^5D_4$ energy level for different concentrations of Tb^{3+}-doped LCZSFB glasses. Inset depicts the fluorescence spectra originating from $^5D_3$ energy level.

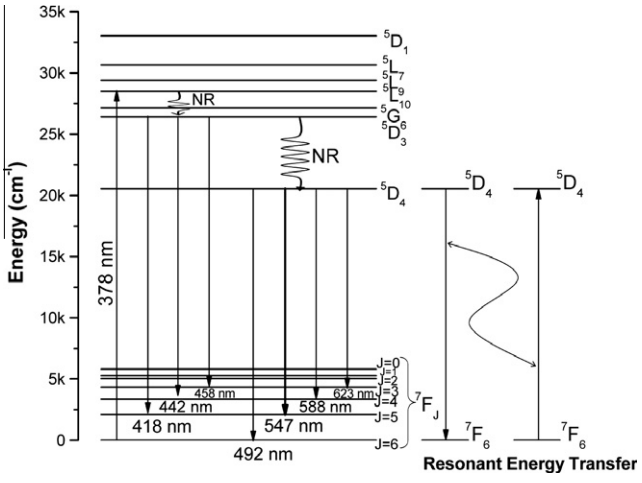

Fig. 8. Partial energy level diagram for Tb^{3+} ions in LCZSFB glasses.

luminescence to be more stable and sustainable display performance for its applications as the green luminescent optoelectronic material. The optical gain parameter ($\sigma_e \times \tau_m$) is also useful to select a laser host material with high stability [57]. In the present investigation, for 1.0 mol% Tb^{3+}-doped LCZSFB glass the optical gain parameter is found to be 21.49×10^{-25} cm^2 s. The fluorescence pattern of Tb^{3+} changes with its contents, i.e., the intensity of respective emission lines can be modified by varying the glass compositions. Green emission is observed for the compounds containing Tb^{3+} in high content, where as the blue emission is observed for that in low content of Tb^{3+} [58,59]. From the above analysis it is observed that the bright green emission from Tb^{3+} is used for the phosphor of fluorescent light and the chromaticity parameters of the present glass can be tuned and is important for the glasses used in LED.

Table 4
Peak emission wavelength (λ_p), effective line width ($\Delta\lambda_p$, nm), radiative transition probabilities (A_R, s^{-1}), total radiative transition probability (A_T, s^{-1}), radiative lifetimes (τ_R, ms), calculated branching ratios (β_R), experimental branching ratios (β_m), stimulated emission cross-section ($\sigma_e \times 10^{-22}$ cm^2) and optical gain parameters ($\sigma_e \times \tau_m$) $\times 10^{-25}$ cm^2 s) for 1.0 mol% Tb^{3+}-doped LCZSFB glass.

Transition		λ_P (nm)	$\Delta\lambda_P$	A_R	β_R	β_m	σ_e	$\sigma_e \times \tau_m$
$^5D_4 \rightarrow$	$^7F_6$	492	13.88	47	0.094	0.398	1.04	1.45
	$^7F_5$	547	12.00	395	0.790	0.547	15.46	21.49
	$^7F_4$	588	10.49	14	0.028	0.043	0.84	1.17
	$^7F_3$	623	7.11	44	0.086	0.012	4.80	6.66
				A_T = 500	τ_R = 2.00			

3.7. Color coordinates

The luminescence color of the samples excited at 378 nm has been characterized by the CIE 1931 chromaticity diagram [7,60]. The emission obtained from Tb^{3+} ions is green in color. The color coordinates (x, y) calculated are found to be (0.34, 0.45) as indicated in Fig. 9. For all the Tb^{3+}:LCZSFB glasses, the color coordinates (0.34, 0.44) located just aside of the pure white color source coordinates (0.33, 0.33) located at the center of the diagram as shown in Fig. 9. This implies that the light emitted by Tb^{3+} ions embedded in LCZSFB glasses is not perfect white light but possess the dominant wavelength deviating from its white light emitting property. The dominant wavelength is determined by drawing a straight line from pure white light coordinates i.e., equal energy point (0.33, 0.33) to the color coordinates of Tb^{3+} ions emission in LCZSFB glasses. The intersection point (0.36, 0.62) is the dominant wavelength (558 nm) of the Tb^{3+} ions emission in LCZSFB glasses. Therefore the emission obtained from Tb^{3+} ions is green in color. The color purity of 558 nm wavelength is 0.91 (91%). Though the emission of Tb^{3+}: LCZSFB glasses are dominant at 558 nm, the color coordinates falls in the white light region as shown in Fig. 9.

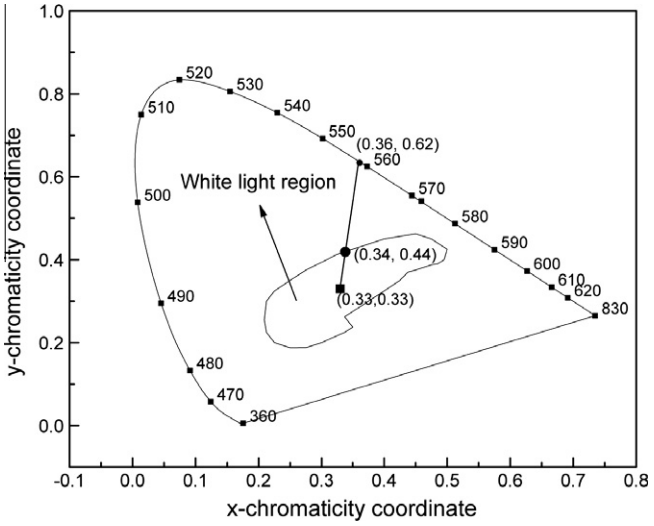

Fig. 9. CIE chromaticity diagram for Tb^{3+} ions in LCZSFB glasses.

3.8. Decay curve analysis

Fluorescence decay curve analysis is very useful for understanding the energy transfer mechanism and quenching behavior of luminescence of Tb^{3+} ions. The lifetime of $^5D_4$ fluorescent level has been measured at room temperature for the glass samples containing 0.5, 1.0, 1.5 and 2.0 mol% of Tb^{3+} ions in LCZSFB glasses by controlling the emission at 547 nm corresponding to $^5D_4 \rightarrow {}^7F_5$ transition upon excitation at 378 nm as shown in Fig. 10. The measured lifetimes (τ_m) of excited $^5D_4$ fluorescent level have been determined by taking the first e-folding times of the decay curves. It is observed that the lifetime is strongly depends upon the Tb^{3+} ion concentration. In lower concentration sample (0.1 and 0.5 mol%), the decay curve shown in Fig. 10 is well fitted to a nearly single exponential which indicates the absence of energy transfer among the Tb^{3+} ions and the lifetime of the emitted level can be calculated using the equation [61], $I(t) = I_0 \exp(\frac{-t}{\tau_0})$, where I_0 is a constant, $I(t)$ is the fluorescence intensity, t is the time after excitation and τ_0 is the intrinsic lifetime of the donors in the absence of acceptors. However, for the samples with higher concentrations (1.0, 1.5 and 2.0 mol%), the fluorescence decay becomes non-exponential due to non-radiative resonant energy transfer between the $^5D_4$ and $^7F_6$ levels of the excited Tb^{3+} ions as shown in Fig. 8.

Table 5
Variation of lifetime (τ_m, ms), quantum efficiency (η, %) and energy transfer rate (W_{ET}, s^{-1}) with respect to concentration (mol%) of Tb^{3+} ions in LCZSFB glasses.

Concentration	Lifetime(ms)	η	W_{ET}
0.10	1.89	94	29
0.50	1.68	84	95
1.00	1.39	70	219
1.50	1.30	65	270
2.00	1.12	55	393

In the present glasses, the measured lifetimes are 1.89, 1.68, 1.39, 1.30 and 1.12 ms for 0.1, 0.5, 1.0, 1.5 and 2.0 mol% of Tb^{3+}. The lifetimes for 1.0 mol% Tb^{3+}-doped glass is comparable to the other reported values [36,56,62,63]. The measured lifetime of excited states τ_m significantly decreases with increase of Tb^{3+} ion concentration due to resonant energy transfer as presented in Table 5. The decrease of lifetime and the departure from the exponential law are characteristic of the existence of a concentration quenching mechanism in the lifetime of $^5D_4$ level at higher concentrations. The τ_m values are significantly smaller than the predicted values (τ_R = 2.0 ms) obtained using the J–O theory. These drastic changes may be due to resonant energy transfer but not due to the multi phonon relaxation because the energy gap between the emitting level ($^5D_4$) and the next lower level ($^7F_0$) is very high about 14,000 cm^{-1}, the multi phonon rate can be neglected. The magnitude of resonant energy transfer rate can be calculated by using the equation $W_{ET} = \frac{1}{\tau_m} - \frac{1}{\tau_R}$ s^{-1}. For the $^5D_4$ level of 1.0 mol% Tb^{3+}-doped LCZSFB glass the resonant energy transfer rate is 219 s^{-1}, which indicates high non-exponential nature of decay

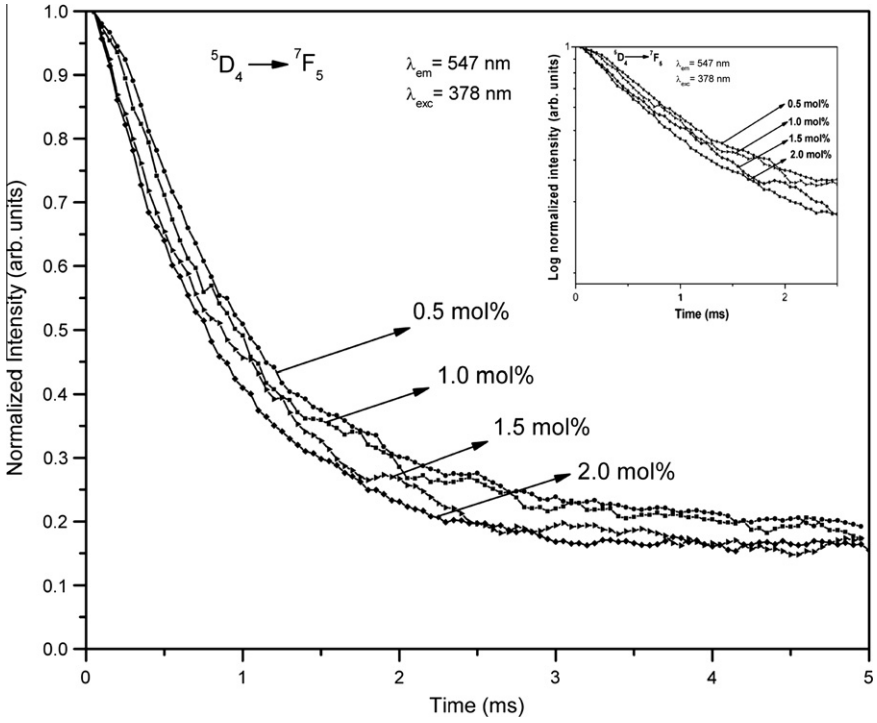

Fig. 10. The decay profiles of $^5D_4 \rightarrow {}^7F_5$ level for different concentrations of Tb^{3+} ions in LCZSFB glasses.

curves at higher concentrations. Reasonably larger values of W_{ET} for higher concentrations ($\geqslant$1.0 mol%) of Tb^{3+} indicate high non-exponential behavior of decay curves. The quantum efficiency ($\eta = \frac{\tau_m}{\tau_R} \times 100\%$) is one of the laser characteristic parameter to predict a laser active medium [64] and is defined as the ratio of the number of photons emitted to the number of photons absorbed. The quantum efficiency for 1.0 mol% Tb^{3+}-doped LCZSFB glass is estimated to be 70% and is comparable to other reported values [36] and for remaining concentrations, the values are noted in Table 5. Thus the reasonably high quantum efficiency of 70% for $^5D_4 \rightarrow {}^7F_5$ laser transition of 1.0 mol% Tb^{3+}-doped LCZSFB glass indicates its utility for green luminescence at 545 nm.

4. Conclusions

In summary, it could be concluded that a series of LCZSFB optical glasses for different concentrations of Tb^{3+} ions have successively been prepared by a melt quenching technique. DSC, FT-IR, FT-Raman, optical absorption, photoluminescence and decay curve spectra were recorded and analyzed by using the Judd–Ofelt theory. The FT-IR and FT-Raman data indicate the presence of trigonal BO_3 and tetrahedral BO_4 structural units in the glasses, the network structure being mainly built by: di-, tri-, tetra-, penta- and ortho-borate groups. From the analysis of optical absorption and fluorescence studies, the J–O intensity parameters, radiative transition rates, branching ratios, radiative lifetimes, stimulated emission cross sections are calculated and are found to be comparable with other reported values. The photoluminescence spectra of the Tb^{3+}:LCZSFB glasses show that the concentration of Tb^{3+} ions increases the intensities of emission peaks originating from $^5D_4$ state also increase. The CIE chromaticity color coordinates calculated for the emission spectra of present glasses show that the glasses emit near white light. The dominant wavelength evaluated from the color coordinates is in the green region and coincides with the most intense transition $^5D_4 \rightarrow {}^7F_5$ (547 nm) of Tb^{3+} ions in LCZSFB glasses. In the present glasses, lifetime of the $^5D_4$ level has been found to be decrease with increasing concentrations of Tb^{3+} ions. At lower concentrations the decay curves are perfectly single exponential and become non-exponential for higher concentrations. The decrease of lifetime at higher concentrations may be due to the resonant energy transfer. Based on the various spectroscopic and emission results such as strong visible emissions, high branching ratios and quantum efficiencies, it is suggested that the 1.0 mol% Tb^{3+} ions doped LCZSFB glasses may be used as luminescent novel optical material for the development of lasers and photonic devices to emit intense green fluorescence at 547 nm corresponding to $^5D_4 \rightarrow {}^7F_5$ transition.

Acknowledgements

The authors are acknowledging the Sophisticated Analytical Instrument Facility (SAIF), Indian Institute of Technology, Chennai for extending instrumental facilities.

References

[1] N. Jaba, H.B. Mansour, A. Kanoun, A. Brenier, B. Champagnon, J. Lumin. 129 (2009) 270.
[2] P. Nandi, G. Jose, Physica B 381 (2006) 66.
[3] S. Tanabe, S. Yoshi, K. Hirao, N. Soga, Phys. Rev. B 45 (1992) 4620.
[4] M. Nakazawa, Y. Kimura, K. Suzuki, Appl. Phys. Lett. 54 (1989) 295.
[5] H. Berthou, C.K. Jorgensen, Opt. Lett. 15 (1990) 1100.
[6] P. Xie, T.R. Gosnell, Opt. Lett. 20 (1995) 1014.
[7] S. Liu, G. Zhao, X. Lin, H. Ying, J. Liu, J. Wang, G. Han, J. Solid State Chem. 181 (2008) 2725.
[8] S. Liu, G. Zhao, H. Ying, J. Wang, G. Han, Opt. Mater. 31 (2008) 47.
[9] W.A. Pisarski, T. Goryczka, B. Wodecka-Dus, M. Plonska, J. Pisarska, Mater. Sci. Eng. B 122 (2005) 94.
[10] V. Venkatramu, P. Babu, C.K. Jayasankar, Spectrochim. Acta A 63 (2006) 276.
[11] W.A. Pisarski, J. Pisarska, G. Dominiak-Dzik, M. Maczka, W. Ryba-Romanowski, J. Phys. Chem. Solids 67 (2006) 2452.
[12] C. Madhukar Reddy, G.R. Dillip, K. Mallikarjuna, J. Lumin. 131 (2011) 1368.
[13] V. Venkatramu, D. Navarro-Urrios, P. Babu, C.K. Jayasankar, V. Lavin, J. Non-Cryst. Solids 351 (2005) 929.
[14] K. Lu, N.K. Dutta, J. Appl. Phys. 91 (2002) 576.
[15] L. Zhang, H.F. Hu, J. Non-Cryst. Solids 292 (2001) 108.
[16] H.B. Yin, P.Z. Deng, J.Z. Zhang, J. Non-Cryst. Solids 210 (1997) 243.
[17] G.M. Kumar, D.N. Rao, Opt. Mater. 31 (2009) 1343.
[18] H. Nakagawa, K. Ebisu, M. Zhang, M. Kitaura, J. Lumin. 102–103 (2003) 590.
[19] F.S. Kao, T.M. Chen, J. Lumin. 96 (2002) 261.
[20] J.G. Kang, J.P. Hong, S.K. Yoon, J.H. Bae, Y.D. Kim, J. Alloys Compd. 339 (2002) 248.
[21] R. Lebullenger, L.A.O. Nunes, A.C. Hernandes, J. Non-Cryst. Solids 284 (2001) 55.
[22] J. Zhang, J. Qiu, Y. Kawamoto, Mater. Lett. 55 (2002) 77.
[23] N. Syam Prasad, K.B.R. Varma, Mater. Sci. Eng. B90 (2002) 246.
[24] S.G. Motke, S.P. Yawale, S.S. Yawale, Bull. Mater. Sci. 25 (2002) 75.
[25] G. Lakshminarayana, S. Buddhudu, Spectrochim. Acta A 62 (2005) 364.
[26] A.G. Souza Filho, J. Mendis Filho, F.E.A. Melo, M.C.C. Custodio, R. Lebullenger, A.C. Hernandes, J. Phys. Chem. Solids 61 (2000) 1535.
[27] B.P. Dwivedi, B.N. Khanna, J. Phys. Chem. Solids 56 (1995) 39.
[28] D. Maniu, T. Iliescu, I. Aredelen, S. Cinta-Pinzaru, N. Tarcea, W. Kiefer, J. Mol. Struct. 651–653 (2003) 485.
[29] C.N. Santos, D.D.S. Meneses, P. Echegut, D.R. Neuville, A.C. Hernandes, A. Lbanez, Appl. Phys. Lett. 94 (2009) 151901.
[30] W.A. Pisarski, J. Pisarska, M. Maczka, W. Ryba-Romanowski, J. Mol. Struct. 792–793 (2006) 207.
[31] R.K. Brow, D.R. Tallant, J. Am. Ceram. Soc. 80 (1997) 1239.
[32] W.T. Carnall, P.R. Fields, K. Rajnak, J. Chem. Phys. 49 (1968) 4424.
[33] J.S. Ofelt, J. Chem. Phys. 49 (1962) 4774.
[34] B.R. Judd, Phys. Rev. B 127 (1962) 750.
[35] G.S. Ofelt, J. Chem. Phys. 37 (1962) 511.
[36] G. Amarnath, S. Buddhudu, J. Non-Cryst. Solids 122 (1990) 66.
[37] P.K.D. Sagar, P. Kistaiah, B.A. Rao, C.V.V. Reddy, K.S.N. Moorthy, N. Veeraiah, J. Mater. Sci. Lett. 18 (1999) 55.
[38] W.T. Carnall, J.P. Hessler, F. Wagner, J. Phys. Chem. 82 (1978) 2152.
[39] H. Takabe, Y. Nageno, K. Morinaga, J. Am. Chem. Soc. 77 (1994) 2132.
[40] R.D. Peacock, Strut. Bond 22 (1975) 83.
[41] W.F. Krupke, Phys. Rev. 145 (1966) 325.
[42] T. Hayakawa, N. Kamata, K. Yamada, J. Lumin. 68 (1996) 179.
[43] C.H. Kam, S. Buddhudu, Physica B 344 (2004) 182.
[44] Z. Xu, Y. Li, Z. Liu, D. Wang, J. Alloys Compd. 391 (2005) 202.
[45] N.S. Hussain, Y.P. Reddy, S. Buddhudu, Mater. Lett. 48 (2001) 303.
[46] V. Aruna, S. Buddhudu, Mater. Lett. 36 (1998) 24.
[47] K. Tonooka, O. Nishimura, J. Lumin. 87–89 (2000) 679.
[48] J. Qiu, M. Shojiya, R. Kanno, Y. Kawamoto, Opt. Mater. 13 (1999) 319.
[49] S. Nishibu, T. Nishio, S. Yonezawa, M. Takashima, J. Lumin. 126 (2007) 365.
[50] Z. Yan, X. Zhongzi, L. Chunhua, N. Yaru, J. Rare Earths 25 (2007) 345.
[51] A.D. Sontakke, K. Biswas, K. Annapurna, J. Lumin. 129 (2009) 1347.
[52] S.V.G.V.A. Prasad, M. Srinivasa Reddy, V. Ravi Kumar, N. Veeraiah, J. Lumin. 127 (2007) 637.
[53] B. Karthikeyan, S. Mohan, M.L. Baesso, Physica B 337 (2003) 249.
[54] S. Rai, S. Hazarika, Opt. Mater. 30 (2008) 1343.
[55] G. Lakshminarayana, J. Qiu, M.G. Brik, I.V. Kityk, J. Phys. Condens. Matter 20 (2008) 375101.
[56] A. Thulasiramudu, S. Buddhudu, Spectrochim. Acta A 66 (2007) 323.
[57] M. Liao, Z. Duan, L. Hu, Y. Fang, L. Wen, J. Lumin. 126 (2007) 139.
[58] H. Huang, B. Yan, Mater. Sci. Eng. B 117 (2005) 261.
[59] Y. Ji, D. Jiang, J. Shi, Mater. Lett. 59 (2005) 868.
[60] P. Babu, K.H. Jang, E.S. Kim, L. Shi, H.J. Seo, F. Rivera-Lopez, U.R. Rodriguez-Mendiza, V. Lavin, R. Vijaya, C.K. Jayasankar, L. Rama Moorthy, J. Appl. Phys. 105 (2009) 013516.
[61] L. Huang, X. Wang, H. Lin, X. Liu, J. Alloys Compd. 316 (2001) 256.
[62] K.K. Mahato, S.B. Rai, Spectrochim. Acta A 56 (2000) 2333.
[63] K.V. Raju, S. Sailaja, C.N. Raju, B.S. Reddy, Spectrochim. Acta A 79 (2011) 87.
[64] V.K. Rai, S.B. Rai, J. Solid State Commun. 132 (2004) 647.